Simplicial Quantum Gravity
Simulations

Andrzej Görlich

Niels Bohr Institute, University of Copenhagen

CERN, July 4rd, 2016

What is Causal Dynamical Triangulation?

Causal Dynamical Triangulation (CDT) is a background independent approach to quantum gravity.

$$\int \mathrm{D}[g] e^{i S^{EH}[g]} \quad \rightarrow \quad \sum_{\mathcal{T}} e^{-S^{R}[\mathcal{T}]}$$

CDT provides a lattice regularization of the formal gravitational path integral via a sum over causal triangulations.

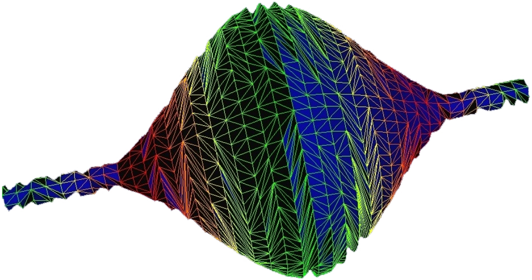

Path integral formulation of quantum mechanics

- A classical particle follows a unique trajectory.
- *Quantum mechanics* can be described by *Path Integrals*: All possible trajectories contribute to the transition amplitude.
- To define the functional integral, we discretize the time coordinate and approximate any path by linear pieces.

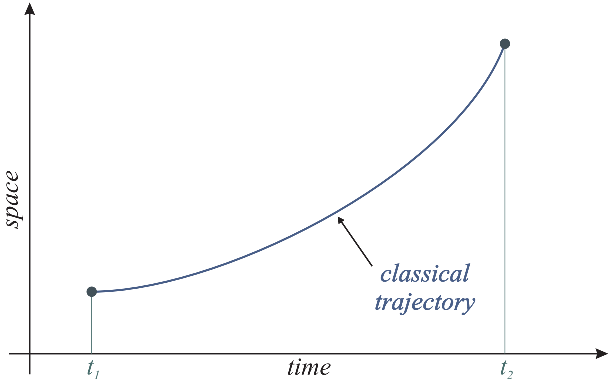

Path integral formulation of quantum mechanics

- A classical particle follows a unique trajectory.
- *Quantum mechanics* can be described by *Path Integrals*: All possible trajectories contribute to the transition amplitude.
- To define the functional integral, we discretize the time coordinate and approximate any path by linear pieces.

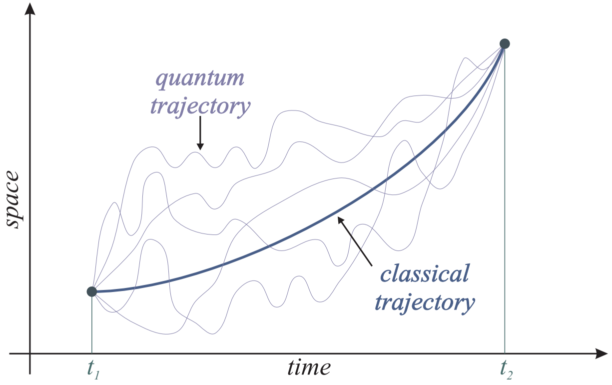

Path integral formulation of quantum mechanics

- A classical particle follows a unique trajectory.
- *Quantum mechanics* can be described by *Path Integrals*: All possible trajectories contribute to the transition amplitude.
- To define the functional integral, we discretize the time coordinate and approximate any path by linear pieces.

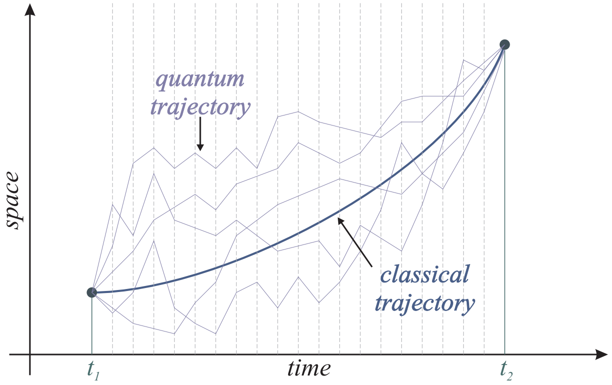

Path integral formulation of quantum gravity

- General Relativity: gravity is encoded in space-time geometry.
- The role of a trajectory plays now the geometry of four-dimensional space-time.
- All space-time histories contribute to the transition amplitude.

1+1D Example: State of system: one-dimensional spatial geometry

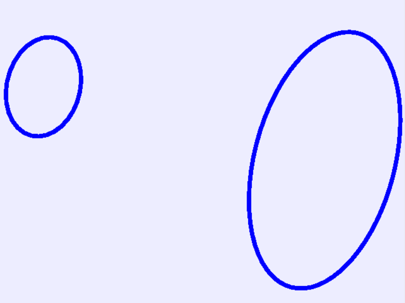

Path integral formulation of quantum gravity

- General Relativity: gravity is encoded in space-time geometry.
- The role of a trajectory plays now the geometry of four-dimensional space-time.
- All space-time histories contribute to the transition amplitude.

1+1D Example: Evolution of one-dimensional closed universe

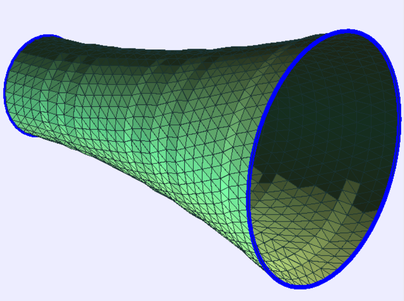

Path integral formulation of quantum gravity

- General Relativity: gravity is encoded in space-time geometry.
- The role of a trajectory plays now the geometry of four-dimensional space-time.
- All space-time histories contribute to the transition amplitude.

Sum over all two-dimensional surfaces joining the in- and out-state

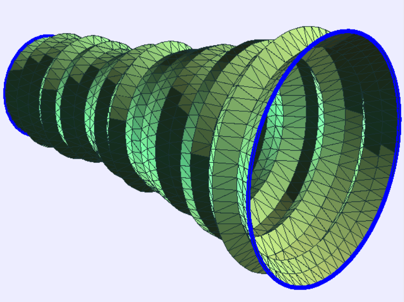

Regularization by triangulation

Dynamical **T**riangulations uses one of the standard regularizations in QFT: **discretization**.

- One-dimensional **state** with a topology S^1 is built from *links* with length a. 2D **space-time** surface is built from equilateral triangles.
- **Curvature** (angle defcit) is localized at vertices.

Example in 2D

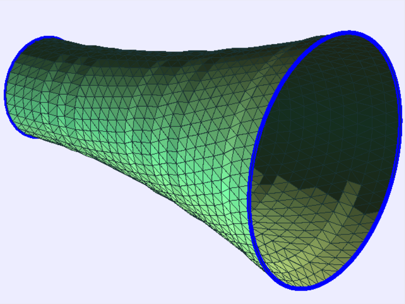

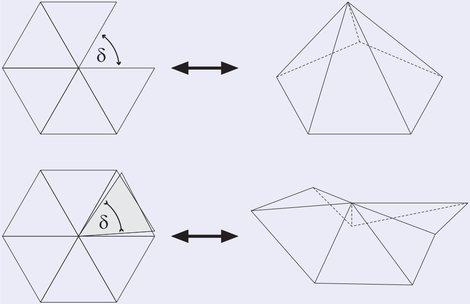

Fundamental building blocks of CDT

- A 4D simplicial manifold is obtained by gluing pairs of 4-simplices (generalization of a triangle) along their 3-faces.
- Length of time links a_t and space links a_s is constant.
- The metric is **flat** inside each 4-simplex. Curvature is localized at triangles. There are two types of simplices.

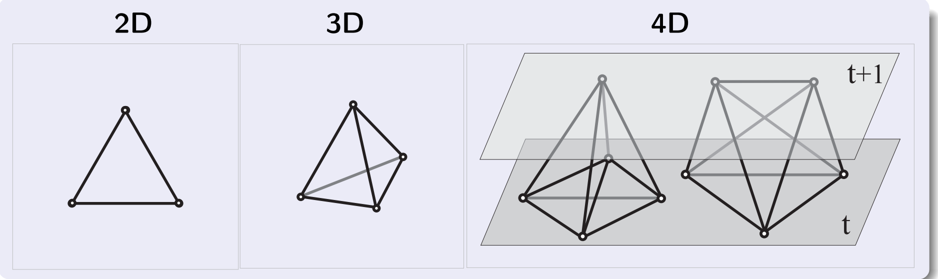

Regge action in four dimensions

The Einstein-Hilbert action has a natural realization on piecewise linear geometries called Regge action

$$S^E[g] = -\frac{1}{G}\int \mathrm{d}t \int \mathrm{d}^D x \sqrt{g}(R - 2\Lambda)$$

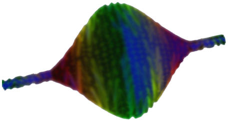

$$\Downarrow$$

$$S^R[\mathcal{T}] = -K_0 N_0 + K_4 N_4 + \Delta(N_{14} - 6N_0)$$

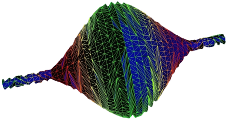

N_0 number of vertices

N_4 number of simplices

N_{14} number of simplices of type $\{1, 4\}$

K_0 K_4 Δ bare coupling constants $(G, \Lambda, \alpha = a_t/a_s)$

Causal Dynamical Triangulations

- The partition function of quantum gravity is defined as a formal integral over all geometries weighted by the Einstein-Hilbert action.

$$Z = \int \mathrm{D}[g] e^{iS^{EH}[g]}$$

- To make sense of the gravitational path integral one uses the standard method of regularization - discretization.
- The path integral is written as a nonperturbative sum over all causal triangulations $\mathcal{T}$.
- Wick rotation is well defined due to global proper-time foliation. $(a_t \rightarrow ia_t)$
- Using **Monte Carlo** techniques we can approximate expectation values of observables.

Causal Dynamical Triangulations

- The partition function of quantum gravity is defined as a formal integral over all geometries weighted by the Einstein-Hilbert action.

$$Z = \sum_{\mathcal{T}} e^{iS^R[g[\mathcal{T}]]}$$

- To make sense of the gravitational path integral one uses the standard method of regularization - discretization.
- The path integral is written as a nonperturbative sum over all causal triangulations $\mathcal{T}$.
- Wick rotation is well defined due to global proper-time foliation. $(a_t \to i a_t)$
- Using **Monte Carlo** techniques we can approximate expectation values of observables.

Causal Dynamical Triangulations

- The partition function of quantum gravity is defined as a formal integral over all geometries weighted by the Einstein-Hilbert action.

$$Z = \sum_{\mathcal{T}} e^{-S^R[\mathcal{T}]}$$

- To make sense of the gravitational path integral one uses the standard method of regularization - discretization.
- The path integral is written as a nonperturbative sum over all causal triangulations $\mathcal{T}$.
- Wick rotation is well defined due to global proper-time foliation. $(a_t \to i a_t)$
- Using **Monte Carlo** techniques we can approximate expectation values of observables.

Causal Dynamical Triangulations

- The partition function of quantum gravity is defined as a formal integral over all geometries weighted by the Einstein-Hilbert action.

$$Z = \sum_{\mathcal{T}} e^{-S^R[\mathcal{T}]}$$

- To make sense of the gravitational path integral one uses the standard method of regularization - discretization.
- The path integral is written as a nonperturbative sum over all causal triangulations $\mathcal{T}$.
- Wick rotation is well defined due to global proper-time foliation. $(a_t \to i a_t)$
- Using **Monte Carlo** techniques we can approximate expectation values of observables.

Numerical setup

- **Monte Carlo** algorithm probes the space of configurations with the probability $P[\mathcal{T}] = \frac{1}{Z} e^{-S[\mathcal{T}]}$.
- To calculate the **expectation value of an observable**, we approximate the path integral by a sum over a finite set of Monte Carlo configurations

$$
\begin{aligned}
\langle \mathcal{O}[g] \rangle &= \frac{1}{Z} \int \mathcal{D}[g] \mathcal{O}[g] e^{-S[g]} \\
&\downarrow \\
\langle \mathcal{O}[\mathcal{T}] \rangle &= \frac{1}{Z} \sum_{\mathcal{T}} \mathcal{O}[\mathcal{T}] e^{-S[\mathcal{T}]} \\
&\downarrow \\
\langle \mathcal{O}[\mathcal{T}] \rangle &\approx \frac{1}{K} \sum_{i=1}^{K} \mathcal{O}[\mathcal{T}^{(i)}]
\end{aligned}
$$

Monte Carlo simulations - Pachner moves

- Initial space-time manifold with given topology
- Random walk over configuration space
- Ergodicity all possible configurations can be generated by moves
- Fixed topology moves don't change the topology
- Causality moves preserve the foliation
- 4D CDT set of 7 moves

Moves in 2D

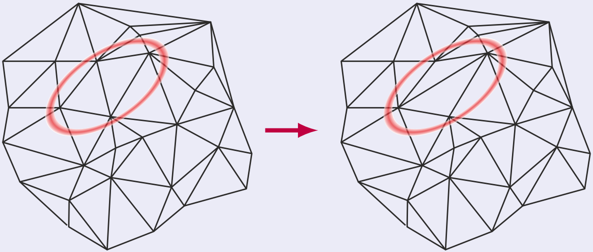

Monte Carlo simulations - Pachner moves

- Initial space-time manifold with given topology
- Random walk over configuration space
- Ergodicity — all possible configurations can be generated by moves
- Fixed topology — moves don't change the topology
- Causality — moves preserve the foliation
- 4D CDT — set of 7 moves

Moves in 3D

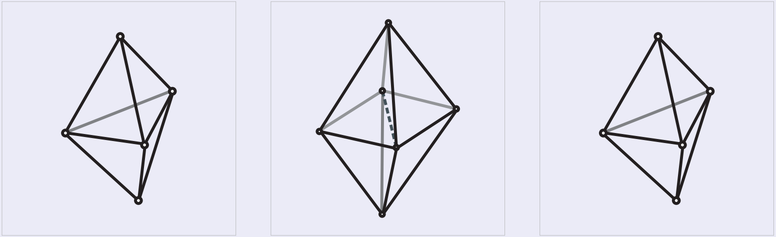

Monte Carlo simulations - Pachner moves

- Initial space-time manifold with given topology
- Random walk over configuration space
- Ergodicity — all possible configurations can be generated by moves
- Fixed topology — moves don't change the topology
- Causality — moves preserve the foliation
- 4D CDT — set of 7 moves

Moves in 3D

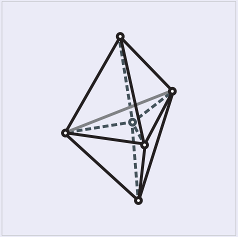

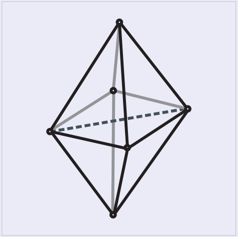

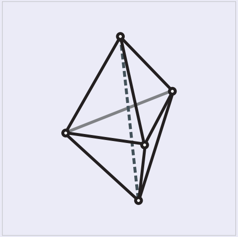

Monte Carlo Markov Chain

- We perform a random walk in the phase-space of configurations (space of piecewise linear geometries).
- Each step is one of the 4D CDT moves.
- The weight (acceptance probability) $W(\mathcal{A} \to \mathcal{B})$ of a move from configuration $\mathcal{A}$ to $\mathcal{B}$ is determined (not uniquely) by the detailed balance condition:

$$P(\mathcal{A})W(\mathcal{A} \to \mathcal{B}) = P(\mathcal{B})W(\mathcal{B} \to \mathcal{A})$$

- The Monte Carlo algorithm ensures that we probe the configurations with the probability $P(\mathcal{A})$.
- After sufficiently long time, the configurations are independent.
- All we need, is the probability functional for configurations $P(\mathcal{A})$ up to the normalization.

Progress since last year meeting

- Previously, our CDT code had used the Knuth's subtractive random number generator **ran3** (lagged Fibonacci).
- For last year MIXMAX RNG has been incorporated into all new code.
- Interested in comparison of **MIXMAX** and **Ran3**: tests, CDT
- Present some new results ...

Ran3

- Very simple and fast (even no multiplication, can be implemented on floating-points)
- Good quality of random numbers
- Range $[0, 10^9)$

```
v[i]  =  (v[i] - v[(i - 31) mod 55]) mod 10^9;
```

Comparison of Ran3 and MIXMAX - BigCrush

To compare MIXMAX and Ran3 we used TestU01 BigCrush suite of 106 tests[1]:

MIXMAX ($N = 256, s = -1$)

- All tests were passed
- Total CPU time: 2h 44m[2]

Ran3

- 19 tests were failed
- Total CPU time: 2h 42m

Dieharder is a RNG testing suite consisting of 114 tests and consumes c.a. 230GB of RNs (as of 30.06.2015). Output for different generators (weak for p-value $<$ 0.5% or p-value $>$ 99.5%):

Name	No. weak	Name	No. weak
MIXMAX, 61-bits	1-3	ran3, 16 LSB	2
MIXMAX, 32 LSB	5	ran3, 16 MSB	1
MIXMAX, 32 MSB	2	MT19937	1

[1] ∼30-bit precision

[2] Intel Xeon CPU E5-1650v2 @ 3.50GHz

Comparison of Ran3 and MIXMAX - CDT simulations

- The dynamical spacetime lattice itself introduces randomness. Hard to verify RNG quality.
- Vicinity of transition point is most sensitive.
- The RNG speed is insignificant (less than 1% CPU time).

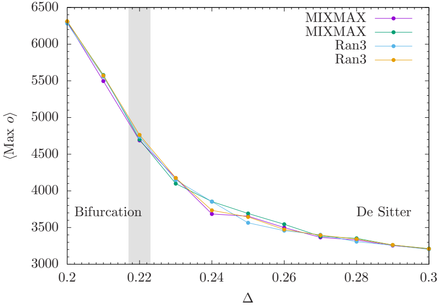

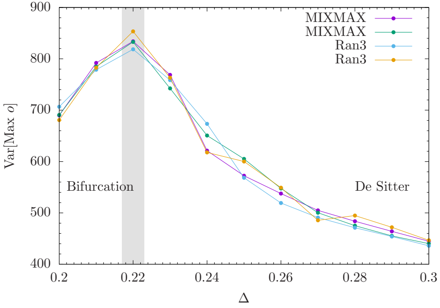

Topology in CDT

- CDT assumes global proper-time foliation of spacetime manifold,
$$\mathcal{M} = \Sigma \times S^1,$$
with Σ being the spatial leaves of foliation.
- Once the topology of spatial slices Σ has been fixed, it is not allowed to change in time (causality condition).
- Time-periodic boundary conditions are chosen for simplicity.
- I will describe differences in outcome between spherical spatial topology ($\Sigma = S^3$) and toroidal spatial topology ($\Sigma = T^3$).

Visualization of foliation and branching

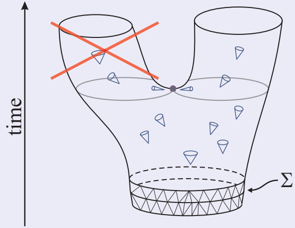

Volume profile

- A basic observable providing information about spacetime geometry is **spatial volume** n_t defined as a number of tetrahedra building a three-dimensional slice $t = 1 \dots T$.
- By **integrating out** (but not "freezing") all degrees of freedom except the scale factor, we restrict our considerations to the spatial volume n_t.
- Indeed, a difference between spherical and toroidal spatial topology is clearly visible in the volume profile.

Spherical

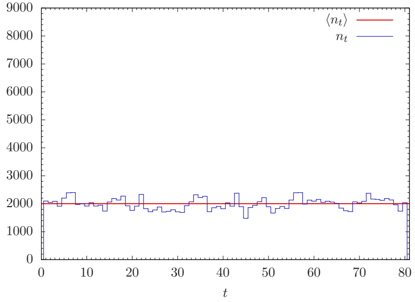

Toroidal

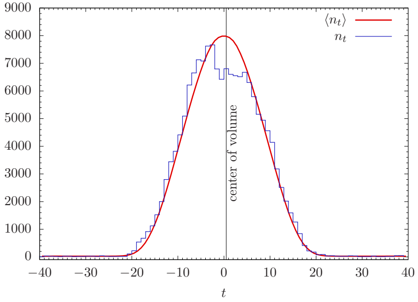

Minisuperspace model

For $\Sigma = S^3$, the average profile and quantum fluctuations of spatial volume are well described by a maximally symmetric model with line element

$$\mathrm{d}s^2 = \mathrm{d}t^2 + a^2(t)\,\mathrm{d}\Omega_3^2, \quad v(t) \propto a^3(t).$$

All degrees of freedom except the scale factor $a(t)$ are „frozen".

$$S_{EH} = \frac{1}{G}\int \mathrm{d}t \int \mathrm{d}\Omega\sqrt{g}(R - 2\Lambda)$$

	Spherical	**Toroidal**
Topology	$S^3 x S^1$	$T^3 x S^1$
$\mathrm{Diag}\, g_{\mu\nu}$	$\{1, a^2, a^2\sin^2 x_2, a^2\sin^2 x_2 \sin^2 x_3\}$	$\{1, a^2, a^2, a^2\}$
Lagrangian $L[a]$	$\frac{1}{\Gamma}a\dot{a}^2 + \mu a - \lambda a^3$	$\frac{1}{\Gamma}a\dot{a}^2 - \lambda a^3$
Lagrangian $L[v]$	$\frac{1}{\Gamma}\frac{\dot{v}^2}{v} + \mu v^{1/3} - \lambda v$	$\frac{1}{\Gamma}\frac{\dot{v}^2}{v} - \lambda v$

Minisuperspace model

For $\Sigma = S^3$, the average profile and quantum fluctuations of spatial volume are well described by a maximally symmetric model with line element

$$\mathrm{d}s^2 = \mathrm{d}t^2 + a^2(t)\,\mathrm{d}\Omega_3^2, \quad v(t) \propto a^3(t).$$

All degrees of freedom except the scale factor $a(t)$ are „frozen".

$$S_{EH} = \frac{1}{G}\int \mathrm{d}t \int \mathrm{d}\Omega \sqrt{g}\,(R - 2\Lambda)$$

No potential term makes it easier to observe quantum corrections

	Spherical	Toroidal
Topology	$S^3 x S^1$	$T^3 x S^1$
Diag $g_{\mu\nu}$	$\{1, a^2, a^2 \sin^2 x_2, a^2 \sin^2 x_2 \sin^2 x_3\}$	$\{1, a^2, a^2, a^2\}$
Lagrangian $L[a]$	$\frac{1}{\Gamma} a\dot{a}^2 + \mu a - \lambda a^3$	$\frac{1}{\Gamma} a\dot{a}^2 - \lambda a^3$
Lagrangian $L[v]$	$\frac{1}{\Gamma}\frac{\dot{v}^2}{v} + \mu v^{1/3} - \lambda v$	$\frac{1}{\Gamma}\frac{\dot{v}^2}{v} - \lambda v$

Effective transfer matrix

The most efficient way to extract the effective action is via the effective transfer matrix.
The model of Causal Dynamical Triangulations can be defined by a transfer matrix $\mathcal{M}$ labeled by $3\mathrm{D}$ triangulations τ of spatial slices,

$$P^{(T)}(\tau_1, \ldots, \tau_T) \equiv \frac{1}{Z} \langle \tau_1 | \mathcal{M} | \tau_2 \rangle \langle \tau_2 | \mathcal{M} | \tau_3 \rangle \ldots \langle \tau_T | \mathcal{M} | \tau_1 \rangle,$$

$$Z = \sum_{\mathcal{T}} e^{-S^R[\mathcal{T}]} \stackrel{!}{=} \mathrm{Tr} \mathcal{M}^T.$$

Element $\langle \tau_1 | \mathcal{M} | \tau_2 \rangle$ denotes the transition amplitude from state $|\tau_1\rangle$ to $|\tau_2\rangle$. Various results suggest existence of an effective transfer matrix M labeled by spatial volume,

$$P^{(T)}(n_1, \ldots, n_T) = \frac{1}{Z} \langle n_1 | M | n_2 \rangle \langle n_2 | M | n_3 \rangle \ldots \langle n_T | M | n_1 \rangle.$$

Effective transfer matrix

The most efficient way to extract the effective action is via the effective transfer matrix.
The model of Causal Dynamical Triangulations can be defined by a transfer matrix $\mathcal{M}$ labeled by 3D triangulations τ of spatial slices,

$$P^{(T)}(\tau_1, \ldots, \tau_T) \equiv \frac{1}{Z}\langle\tau_1|\mathcal{M}|\tau_2\rangle\langle\tau_2|\mathcal{M}|\tau_3\rangle \ldots \langle\tau_T|\mathcal{M}|\tau_1\rangle,$$

$$Z = \sum_{\mathcal{T}} e^{-S^R[\mathcal{T}]} \stackrel{!}{=} \mathrm{Tr}\mathcal{M}^T.$$

Exact

Property

Element $\langle\tau_1|\mathcal{M}|\tau_2\rangle$ denotes the transition amplitude from state $|\tau_1\rangle$ to $|\tau_2\rangle$. Various results suggest existence of an effective transfer matrix M labeled by spatial volume,

$$P^{(T)}(n_1, \ldots, n_T) = \frac{1}{Z}\langle n_1|M|n_2\rangle\langle n_2|M|n_3\rangle \ldots \langle n_T|M|n_1\rangle.$$

Measurement of the transfer matrix

Decomposition of a distribution probability into a product of transfer matrix elements,

$$P^{(T)}(n_1, \ldots, n_T) \equiv \frac{1}{Z} \langle n_1|M|n_2\rangle \langle n_2|M|n_3\rangle \ldots \langle n_T|M|n_1\rangle,$$

where

$$\langle n|M|m\rangle = \mathcal{N} e^{-L(n,m)},$$

is consistent with a discretized action of the minisuperspace model,

$$L(n,m) = \frac{1}{\Gamma} \frac{(n-m)^2}{n+m} + u(n+m) \longleftarrow L[v] = \frac{1}{G} \frac{\dot{v}^2}{v} + u(v).$$

The simplest way to measure the transfer matrix is to use a system with only $T = 2$ spatial slices. In such case,

$$\langle n|M|m\rangle = \sqrt{P^{(2)}(n,m)}.$$

It is also possible to use a combination of results for $T > 2$.

Measurement of the transfer matrix

Decomposition of a distribution probability into a product of transfer matrix elements,

$$P^{(T)}(n_1, \ldots, n_T) \equiv \frac{1}{Z}\langle n_1|M|n_2\rangle\langle n_2|M|n_3\rangle \ldots \langle n_T|M|n_1\rangle,$$

where

Couples only adjacent slices

$$\langle n|M|m\rangle = \mathcal{N} e^{-L(n,m)},$$

is consistent with a discretized action of the minisuperspace model,

$$L(n,m) = \frac{1}{\Gamma}\frac{(n-m)^2}{n+m} + u(n+m) \;\longleftarrow\; L[v] = \frac{1}{G}\frac{\dot{v}^2}{v} + u(v).$$

The simplest way to measure the transfer matrix is to use a system with only $T = 2$ spatial slices. In such case,

$$\langle n|M|m\rangle = \sqrt{P^{(2)}(n,m)}.$$

Assumption

It is also possible to use a combination of results for $T > 2$.

Effective action

Effective transfer matrix $\langle n|M|m\rangle$

$S^3 \times S^1$

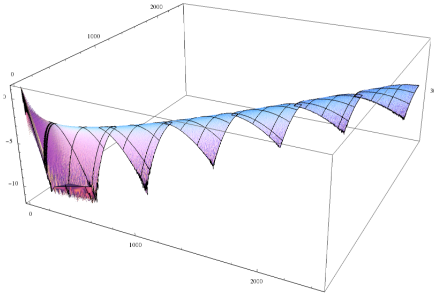

$T^3 \times S^1$

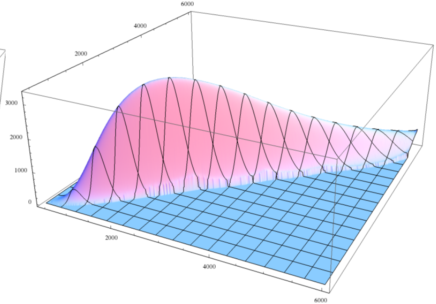

Strong discretization effects for small volumes.

Low probability of small volumes.

Effective action

Potential

$S^3 \times S^1$ $\qquad$ $T^3 \times S^1$

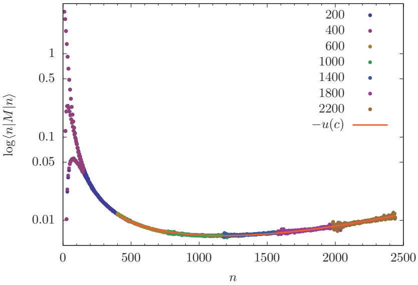

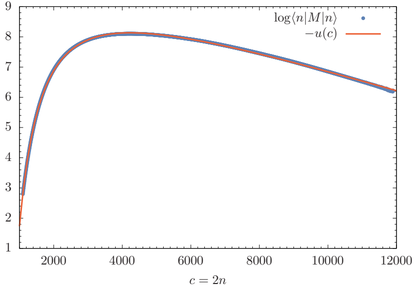

$$u(c) = \mu c^{1/3} - \lambda c \qquad\qquad u(c) = \mu c^{-3/2} + \lambda c$$

Curvature of the potential explains the average volume profile.

Effective action

Potential

$S^3 \times S^1$ $\qquad$ $T^3 \times S^1$

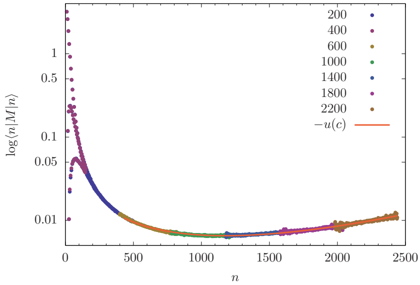

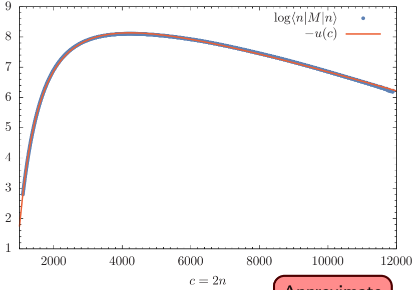

Approximate

$$u(c) = \mu c^{1/3} - \lambda c \qquad\qquad u(c) = \mu c^{-3/2} + \lambda c$$

Curvature of the potential explains the average volume profile.

Volume fixing term necessary for $S^3 \times S^1$

Effective action

Kinetic term

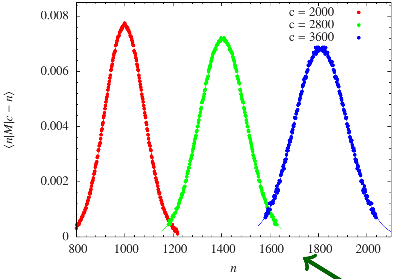

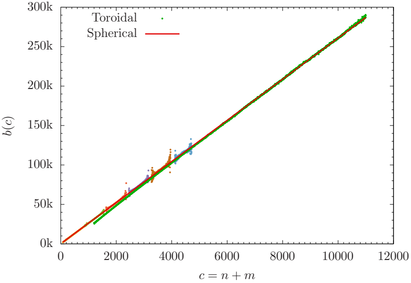

$S^3 \times S^1$

Anti-diagonals form a Gaussian function

$T^3 \times S^1$

$$\langle n|M|m\rangle = e^{-\left[\frac{(n-m)^2}{\Gamma c} + \mu c^{1/3} - \lambda c\right]}$$

$$\langle n|M|m\rangle = e^{-\left[\frac{(n-m)^2}{\Gamma c} + \mu c^{-3/2} + \lambda c\right]}$$

The kinetic term is identical in both cases ($\Gamma \approx 26.3$).

Future work - parallelise and adapt to GPU

- In general it seems difficult to parallelise the CDT MC code.
- Close to transition / triple point acceptance rate is very low (critical slowing down), and a *parallel rejection* algorithm can be applied. (Assembler AVX2 code for spectral dimension).
- Series (block) of random numbers is precomputed and split between threads.

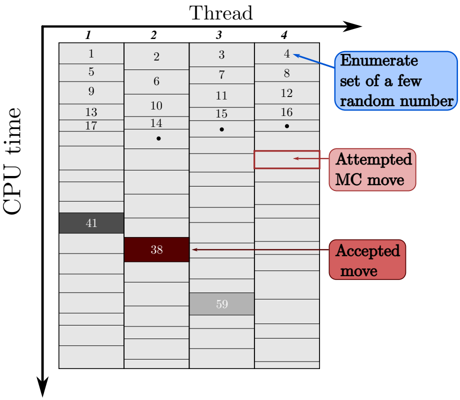

Future work - adapt to GPU

- The next step is to take advantage of GPU multithreading.

  Problems:

- A typical GPU card has 32 threads/warp and 64kB of fast shared memory limit.
- MIXMAX $N = 256$ state vector takes 2kB (64kB / warp). Decrease N? Parameter m?
- Filling an array of random number isn't faster.
- Thread should execute the same commands (move).

- Tested AVX2 version of MIXMAX (intrinsic and asm code)

Summary

- The model of **C**ausal **D**ynamical **T**riangulations is a lattice approach to quantum gravity.
- In 3+1-dimensions it exhibits a different behavior (inside de Sitter phase) for spherical and toroidal spatial topologies.
- For $S^3 \times S^1$ we have a *blob-like* de Sitter solution. For $T^3 \times S^1$ we have a uniform volume profile.
- The difference can be explained by the shape (second derivative) of the effective potential. In both cases the kinetic term is identical.
- MIXMAX performed much better in BigCrush test then previous RNG, but no difference in CDT outcome was observed.
- Plans to parallelise the MC algorithm and adapt to GPU.

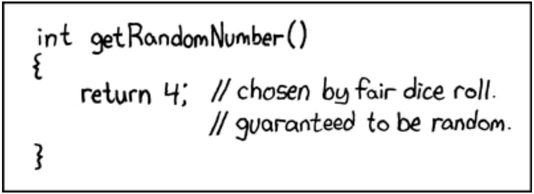

Thank you!

Subtractive random number generator

So far, we used the Knuth's subtractive random number generator **ran3**.

- Very simple and fast (even no multiplication, can be implemented on floating-points)
- Good quality of random numbers
- Range $[0, 10^9)$

```
v[i]  =  (v[i] - v[(i - 31) mod 55]) mod 10^9;
```

MIXMAX

Speed is not important for our purposes

- Fast (slightly slower per number than **ran3** but faster per bit)
- Very good quality of random numbers
- Useful when dealing with double-precision floating-point numbers (53-bit significant precision)
- Passed a set of simple tests (Chi square, 1D Kolmogorov-Smirnoff, n-dim ball, series, collections, etc.) + distributions
- Assembler implementation as fast as C
- No easy way to verctorize a single generator (e.g. using AVX instructions)

I used a version with $N = 256$ and $P = 2^{61} - 1$.
It produces random numbers in a range $0 < x < 2^{61} - \cancel{1}$.
Usually we need and integer random number `i` in a range `0 < i < n`.
This can be easily done without a conversion to floating-point numbers:

```
i = ((unit128_t) n * x) >> 61
```

Futute plan: Use MIXMAX in our Monte-Carlo simulations and check if there is any difference.

Dieharder

Dieharder is a RNG testing suite by Robert Brown.
It consists of 114 tests and consumes c.a. 230GB of RNs[3].
Output for different generators:

Name	No. weak
ran3, 16 LSB	2
ran3, 16 MSB	1
MIXMAX, 61-bits	1-3
MIXMAX, 32 LSB	5
MIXMAX, 32 MSB	2
MT19937	1

Result is **weak** for p-value $< 0.5\%$ or p-value $> 99.5\%$.

[3] As of 30.06.2015

The Ziggurat method

When including matter fields to our simulations, the time of generating Gaussian random numbers becomes important.

- The Marsaglia polar method requires to calculate a *logarithm* and a *square root* every (second) step - slow.

The Ziggurat method is a reject method. It splits the space into a number boxes (e.g. 2^7) of equal areas. It has a very high acceptance rate (>95%) and rarely requires to calculate an *exponent* ($< 3\%$). It is about $3.5\times$ **faster** than the polar method.

The MIXMAX's $61-\mathrm{bits} = 7 + 1 + 53$.